American Research Journal of Dermatology
Volume 1, Issue 1, pp: 1-21

AMERICAN RESEARCH JOURNALS
An Academic Publishing House

Research Article Open Access

Biological Activity of an Essential Oil Blend in Human Dermal Fibroblasts

Xuesheng Han, Tyler Bahr*

dōTERRA International LLC, 389 S. 1300 W. Pleasant Grove, UT 84062, USA

tbahr@doterra.com

Abstract: Research on the biological activities of essential oilsin human skin cells is limited. This study first analyzed the effect of an essential oil blend (EOB) on 17 important protein biomarkers in cytokine-stimulated human dermal fibroblasts. The EOB was composed of essential oils of frankincense resin, sweet orange peel, litsea fruit, thyme plant, clove bud, summer savory plant, and niaouli leaf. The results showed that EOB had excellent antiproliferative activity. It significantly increased vascular cell adhesion molecule 1 levels and slightly increased the monocyte chemoattractant protein 1 and epidermal growth factor receptor production. We then studied the effect of the EOB on the expression levels of 21,224 genes in the same cells. We found that the EOB markedly affected genome-wide gene expression. Further analysis revealed that the EOB pleiotropically regulated multiple signaling pathways in human cells including hepatic fibrosis activation, antigen presentation, mitotic roles of the polo-like kinase, and cyclin and cell cycle regulation. Many pathways significantly affected by the EOB are closely related to inflammatory and immune responses. The results suggest that the EOB may affect biological processes and global gene expression in human skin cells. Further research into the underlying mechanism of action of the EOB is needed.

Keywords: Essential oil; frankincense; sweet orange; litsea; thyme; inflammation; immune response; signaling pathway; tumor; genome-wide gene expression

Introduction

Essential oils are complex mixtures of aromatic compounds naturally produced in plants. They have been used historically as well as currently for treating a variety of diseases and maintaining health in humans (Lv et al., 2013; Perry & Perry, 2006). Recent pre-clinical and clinical studies have provided evidence supporting the benefits of essential oils to human health (Kozioł et al., 2014; Navarra et al., 2015), resulting in a wider acceptance and use of essential oils in the US and worldwide. Despite this trend, very few studies have elucidated the mechanisms of action of essential oils inhuman cells.

Thousands of distinct terpene compounds have been identified in essential oils, many of which are known for possessing diverse biological activities. Because every essential oil is primarily composed of a unique mixture of just a few of these compounds, it is hypothesized that each oilhas its own unique array of biological activities. For example, Oregano essential oil is known to have powerful anti-fungal and anti-microbial effects due to its high phenylpropene content, while Lavender's main constituents, linalool and linalyl acetate, are known to calm the CNS by activating GABAA receptors.

The tendency for essential oil compounds to exhibit synergy and antagonism is another phenomenon that is receiving growing attention. A recent study on membrane dynamics suggested that the ratios of constituents might affect an oil's activity just as much as the identity of the constituents (Hac-Wydro et al., 2017). The possibility of synergy and antagonism has sparked an interest in blending, or creating mixtures of essential oils, to achieve an oil combination with novel effects. Therefore, we studied the biological effect of an industrial essential oil blend (EOB)on a human skin disease model, the HDF3CGF pre-inflamed dermal fibroblast system, which we have used previously to study the effects of individual essential oils. The current findings will allow

comparison of this blend's activity with that of the individual essential oils and possibly other blends, aiding in future research on synergy, antagonism, and additive effects of essential oil blends.

The EOB contains a mixture of essential oils from frankincense (*Boswellia carterii*, *Boswellia frereana*, and *Boswelliasacra*) resin, sweet orange (*Citrus sinensis*) peel, listea (*Litsea cubeba)* fruit, thyme (*Thymus vulgaris*) plant, clove (*Eugenia caryophyllata*) bud, the summer savory (*Satureja hortensis*) plant, and niaouli (*Melaleuca quinquinervia*) leaf. Although many of these individual essential oils and their active constituents are known to have various therapeutic benefits, this was the first study to examine the effect of a commercial blend of these oils on human genome-wide gene expression in the HDF3CGF model system. We also studied the EOB's effect on biomarkers related to inflammation, immune responses, and tissue remodeling.

Materials and Methods

All experiments were conducted using a biologically multiplexed activity profiling (Bio MAP) system HDF3CGF designed to model the pathology of chronic inflammation robustly and reproducibly. The system comprised three components: a cell type, stimuli to create the disease environment, and a set of biomarker (protein) readouts to examine the treatment effects on the disease environment (Berg et al., 2010). The methodologies used in this study were essentially the same as those previously described (Han & Parker, 2017a, 2017b; Kunkel et al., 2004).

Reagents

The EOB (dōTERRA, Pleasant Grove, UT, USA) was diluted in dimethyl sulfoxide (DMSO) to 8× the specified concentrations (final DMSO concentration was no more than 0.1%). Then, 25 µL of each 8× solution was added to the cell culture to a final volume of 200 µL whileDMSO (0.1%) served as the vehicle control.

The composition of the EOB was as follows: frankincense (a mixture of *B. carterii*, *B. frereana*, and *B. sacra*) resin oil, sweet orange (*C. sinensis*) peel oil, litsea (Litsea cubeba) fruit oil, thyme (*T. vulgaris*) plant oil, clove (*E. caryophyllata*) bud oil, summer savory (*S. hortensis*) plant oil, and niaouli (*M. quinquinervia*) leaf oil. The exact percentage composition is proprietary to the supplying company. Aromatic compounds distilled from the plant material comprised 100% of the EOB. Each essential oil originated from a country where the plant is grown. The essential oils were shipped to the US, where they were blended into the EOB. Gas chromatography-mass spectrometry analysis of the EOB showed that it contained 23–27% limonene, 11–14% alpha-pinene, 6–8% eugenol, 6–8% thymol, 5–7% carvacrol, 5–7% eucalyptol, 4–6% gamma-terpinene, and smaller amounts of other aromatic compounds.

Cell Cultures

Primary human neonatal fibroblasts were prepared as previously described (Bergamini et al., 2012) and were plated under low-serum conditions (0.125% fetal bovine serum) for 24 h. Then, the cell culture was stimulated with a mixture of interleukin (IL)-1β, tumor necrosis factor (TNF)-α, interferon (IFN)-Ɣ, basic fibroblast growth factor (bFGF), epidermal growth factor (EGF), and platelet-derived growth factor (PDGF) for another 24 h. The cell culture for the HDF3CGF assays was performed in a 96-well plate,and the stimulation conditions were described in detail elsewhere (Bergamini et al., 2012; R Development Core Team, 2011).

Protein-Based Readouts

An enzyme-linked immunosorbent assay (ELISA) was used to measure the biomarker levels of cell-associated and cell membrane targets. Soluble factors in the supernatants were quantified using either homogeneous time-resolved fluorescence detection, bead-based multiplex immunoassay, or capture ELISA. The adverse effects of the test agents on cell proliferation and viability (cytotoxicity) were measured using the sulforhodamine B (SRB) assay. For proliferation as says, the cells were cultured and measured after 72 h, which is optimal for the HDF3CGF system, and the detailed procedure was described in a previous study (Bergamini et al., 2012). The measurements were performed in triplicate wells, and a glossary of the biomarkers used in this study is provided in Supplementary Table S1.

Table S1. *Glossary of Biomarkers of the Human Dermal Fibroblast System HDF3CGF Used in the Study*

Readout	Description
CCL2/MCP-1	MCP-1 system is a chemokine that mediates recruitment of monocytes and T cells into sites of inflammation. MCP-1 is categorized as an inflammation-related activity in the HDF3CGF system modeling Th1 inflammation involved in wound healing and matrix remodeling.
CD106/VCAM-1	VCAM-1 is a cell adhesion molecule that mediates adhesion of monocytes and T cells to endothelial cells. VCAM-1 is categorized as an inflammation-related activity.
CD54/ICAM-1	ICAM-1 is a cell adhesion molecule that mediates leukocyte-endothelial cell adhesion and leukocyte recruitment. ICAM-1 is categorized as an inflammation-related activity.
Collagen I	Collagen I is involved in tissue remodeling and fibrosis, and is the most common fibrillar collagen that is found in skin, bone, tendons and other connective tissues. Collagen I is categorized as a tissue remodeling-related activity.
Collagen III	Collagen III is an extracellular matrix protein and fibrillar collagen found in extensible connective tissues (skin, lung and vascular system) and is involved in cell adhesion, cell migration, tissue remodeling. Collagen III is categorized as a tissue remodeling-related activity.
CXCL10/IP-10	IP-10 is a chemokine that mediates T cell, monocyte and dendritic cell chemotaxis. IP-10 is categorized as an inflammation-related activity.
CXCL11/I-TAC	I-TAC is a chemokine that mediates T cell and monocyte chemotaxis. I-TAC is categorized as an inflammation-related activity.
CXCL8/IL-8	IL-8 is a chemokine that mediates neutrophil recruitment into acute inflammatory sites. IL-8 is categorized as an inflammation-related activity.
CXCL9/MIG	MIG is a chemokine that mediates T cell recruitment. MIG is categorized as an inflammation-related activity.
EGFR	EGFR is a cell surface receptor for epidermal growth factor involved in cell proliferation during development as well as tumor growth. EGFR is involved in Epithelial cell proliferation, epithelial cell differentiation keratinocyte proliferation, tissue remodeling. EGFR is categorized as a tissue remodeling-related activity.
M-CSF	M-CSF is a secreted and cell surface cytokine that mediates macrophage differentiation. M-CSF is categorized as an immune modulation-related activity.
MMP-1	MMP-1 is an interstitial collagenase that degrades collagens I, II and III and is involved in the process of tissue remodeling. MMP-1 is categorized as a tissue remodeling-related activity.
PAI-I	PAI-I is a serine proteinase inhibitor and inhibitor of tissue plasminogen activator (tPA) and urokinase (uPA) and is involved in tissue remodeling and fibrinolysis. PAI-I is categorized as a tissue remodeling-related activity.
Proliferation_72hr	Proliferation_72hr in the HDF3CGF system is a measure of dermal fibroblast proliferation which is important to the process of wound healing and fibrosis.
SRB	SRB is a measure of the total protein content of dermal fibroblasts. Cell viability of adherent cells is measured by Sulforhodamine B (SRB) staining, a method that determines cell density by measuring total protein content of test wells.
TIMP-1	TIMP-1 is a tissue inhibitor of matrix metalloprotease-7 (MMP-7) and other MMPs, and is involved in tissue remodeling, angiogenesis and fibrosis. TIMP-1 is categorized as a tissue remodeling-related activity.
TIMP-2	TIMP-2 is a tissue inhibitor of matrix metalloproteases and is involved in tissue remodeling, angiogenesis and fibrosis. TIMP-2 is categorized as a tissue remodeling-related activity.

The quantitative biomarker data are presented as the mean $\log_{10}$ relative expression level (compared to their respective mean vehicle control value) ± standard deviation (SD) of triplicate measurements. Differences in biomarker levels between the EOB- and vehicle-treated cultures were tested for significance using the unpaired Student's *t*-test. A p-value < 0.05, outside of the significance envelope, with an effect size of at least 10% (> 0.05 $\log_{10}$ ratio units), was considered statistically significant.

RNA Isolation

Total RNA was isolated from cell lysates using the Zymo*Quick-RNA*M in iPrep kit (Zymo Research Corp., Irvine, CA, USA) according to the manufacturer's instructions. RNA concentration was determined using a Nano Drop ND-2000 system (Thermo Fisher Scientific, Waltham, MA, USA). The RNA quality was assessed using a Bioanalyzer 2100 (Agilent Technologies, Santa Clara, CA, USA) and an Agilent RNA 6000 Nano kit. All samples had an A260/A280 ratio between 1.9 and 2.1 and an RNA integrity number score greater than8.0.

Microarray Analysis of Genome-Wide Gene Expression

The effect of the EOB at a concentration of 0.0033% (v/v) was tested on the expression of 21,224 genes in the HDF3CGF system following a 24-h treatment. Samples for microarray analysis were processed by Asuragen, Inc. (Austin, TX, USA) according to the company's standard operating procedures. Biotin-labeled cRNAwas prepared from 200 ng total RNA using an Illumina TotalPrep RNA amplification kit (Thermo Fisher Scientific, Waltham, MA, USA) and one round of amplification. The cRNA yields were quantified using ultraviolet spectrophotometry, and the distribution of the transcript sizes was assessed using the Agilent Bioanalyzer 2100. Labeled cRNA (750 ng) was used to probe Illumina human HT-12 v4 expression bead chips (Illumina, Inc., San Diego, CA, USA). Hybridization, washing, staining with streptavidin-conjugated cyanine-3, and scanning of the Illumina arrays were carried out according to the manufacturer's instructions. The Illumina BeadScan software was used to produce the data files for each array, and the raw data were extracted using the Illumina Bead Studio software.

The raw data were uploaded into R (R Development Core Team, 2011), and the quality-control metrics was analyzed using the beadarray package (Dunning et al., 2007). The data were normalized using quantile normalization (Bolstad et al., 2003), and then re-annotated and filtered to remove probes that were non specific or mapped to intronic or intragenic regions (Barbosa-Morais et al., 2010). The remaining probe sets comprised the data set for the subsequent analysis. The fold-change expression for each set was calculated as the log2 ratio of EOB to the vehicle control. These fold-change values were uploaded in to the Ingenuity Pathway Analysis (IPA) program (Qiagen, Redwood City, CA, USA, www.qiagen.com/ingenuity) to generate the networks and pathway analyses.

Results and Discussion

Bioactivity Profile of EOB in HDF3CGF System

The HDF3CGF system was designed to model the pathology of chronic inflammation and wound healing in the context of Th1-type inflammation. Four different concentrations (0.01, 0.0033, 0.0011, and 0.0037% v/v) of the EOB were initially tested for cytotoxic activity in the dermal fibroblasts. A concentration of 0.01% was overtly cytotoxic and, therefore, the 0.0033% concentration was usedin the further analysis. Biomarkers were designated if the EOB values were significantly different ($p < 0.05$) from vehicle controls, outside the significance envelope, with an effect size of at least 10% (> 0.05 log ratio units, Figure 1).

Studies by other research groups have shown the anti-inflammatory and immune modulating properties of the major chemical constituents of the EOB, specifically limonene and α-pinene. Topically-applied limonene, the main constituent of orange oil, reduced edema in mouse skin and pretreatment with limonene reduced inflammatory markers (Chaudhary et al., 2012). In RAW 264.7 macrophages, limonene reduced several immune markers including TNF-α (Yoon et al., 2010).Limonene's anti-inflammatory effects in rat kidney tissue were found to be associated with decreased expression of nuclear factor(NF)-κB (Rehman et al., 2014). Mouse

studies demonstrated the anti-inflammatory activities of frankincense oil and α-pinene, andthe effect was likely mediated by reducingnuclear factor NF-κB nuclear translocation (Zhou et al., 2004). The immunomodulatory effect of α-pinene was attributed to the suppression of mitogen-activated protein kinases (MAPKs) and the NF-κB pathway in mouse peritoneal macrophages, which showed decreased expression of TNF-α, NF-κB, and interleukins (Kim et al., 2015).

The individual essential oils in the EOB that we have studied previously include frankincense and clove oils (Han & Parker, 2017c, 2017d). It was interesting to observe that certain biomarker effects from the individual essential oils were conserved in the blend, while others were lost. For instance, we previously found that both frankincense and clove oils significantly inhibit cell proliferation, so it was no surprise that the blend also inhibited cell proliferation. Also noteworthy was the MCP-1 downregulation by the blend, which was not observed after treatment with either of the essential oils previously studied. This difference could be attributed to one of the other oils in the blend or perhaps the unique combination of oils. Finally, the blend had virtually no effect on collagen levels, which were significantly downregulated by frankincense andclove oils. These observations support the hypothesis that the EOB has unique biological activity that may perhaps be more than a simple sum of effects from the individual essential oils included in the blend. One obvious limitation to comparing the blend with these oils, however, is our lack of biomarker data on niaouli, litsea, summer savory, thyme, and orange. Future research will make it possible to conduct a more comprehensive comparison of the effects of the EOB compared to its individualcomponent oils.

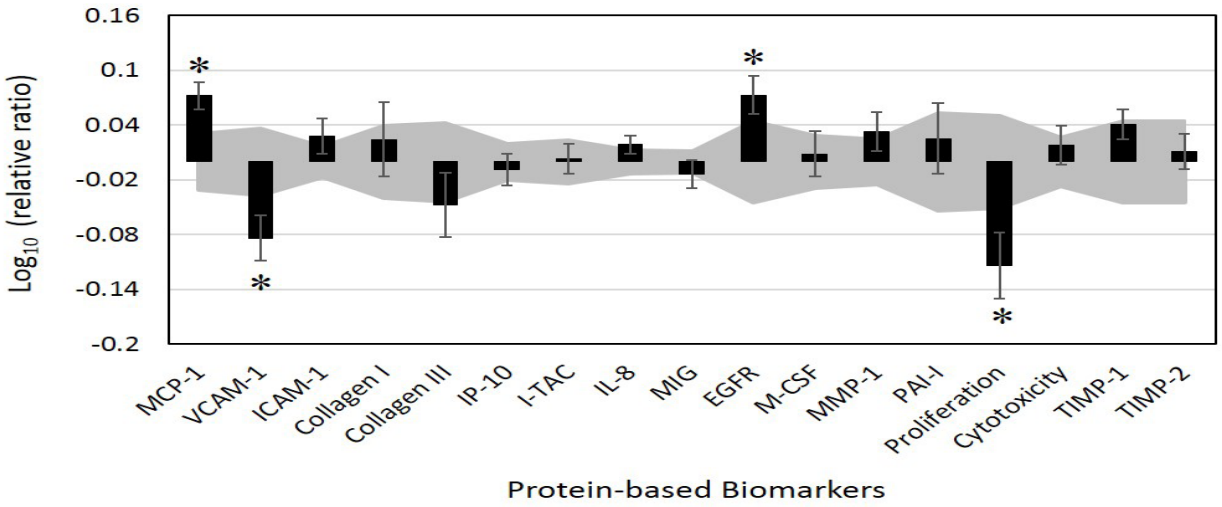

Fig1. *The bioactivity profile of an essential oil blend (EOB, 0.0033% v/v) in a human dermal fibroblast system HDF3CGF. Y-axis denotes the relative expression levels of biomarkers compared to vehicle control values, in log10 form. Error bars represents the standard deviations (SD) of triplicate measurements. Vehicle control values are shaded in gray, denoting the 95% significance envelope. A * indicates a biomarker designated with "key activity," i.e., biomarker values were significantly different ($p < 0.05$) from vehicle controls, outside of the significance envelope, with an effect size of at least 10% (more than 0.05 log ratio units). MCP-1, monocyte chemoattractant protein; VCAM-1, vascular cell adhesion molecule 1; ICAM-1, intracellular cell adhesion molecule 1; IP-10, interferon gamma-induced protein 10; I-TAC, interferon-inducible T-cell alpha chemoattractant; IL-8, interleukin-8; MIG, monokine-induced by interferon-γ; EGFR, epidermal growth factor receptor; M-CSF, macrophage colony-stimulating factor; MMP-1, matrix metalloproteinase 1; PAI-1, plasminogen activator inhibitor 1; TIMP, tissue inhibitor of metalloproteinase*

Effect of EOBon Genome-Wide Gene Expression

To further explore the effect of 0.0033% (v/v) EOB on human skin cells, we analyzed its effect on the RNA expression of 21, 224 genes. The EOB significantly regulated the expression levels of hundreds of genes globally. The vast majority of the 200mostregulated genes (178) were downregulated by the EOB while the rest were upregulated (Table S2 and see **Supplementary Material** for more information).

Table S2. *200 most-impacted genes by the EOB (0.0033% v/v, fold change in log2 ratio form)*

Illumina Gene ID	Fold Change	Definition
AKR1C4	4.38	Homo sapiens aldo-keto reductase family 1, member C4 (chlordecone reductase; 3-alpha hydroxysteroid dehydrogenase, type I; dihydrodiol dehydrogenase 4) (AKR1C4), mRNA.
MMP10	4.13	Homo sapiens matrix metallopeptidase 10 (stromelysin 2) (MMP10), mRNA.
RSAD2	3.87	Homo sapiens radical S-adenosyl methionine domain containing 2 (RSAD2), mRNA.
AKR1C2	3.66	Homo sapiens aldo-keto reductase family 1, member C2 (dihydrodiol dehydrogenase 2; bile acid binding protein; 3-alpha hydroxysteroid dehydrogenase, type III) (AKR1C2), transcript variant 1, mRNA. XM_943424 XM_943425 XM_943427
SLC7A11	3.17	Homo sapiens solute carrier family 7, (cationic amino acid transporter, y+ system) member 11 (SLC7A11), mRNA.
ODC1	2.69	Homo sapiens ornithine decarboxylase 1 (ODC1), mRNA.
TFRC	2.64	Homo sapiens transferrin receptor (p90, CD71) (TFRC), mRNA.
GLDN	2.57	Homo sapiens gliomedin (GLDN), mRNA.
TDO2	2.47	Homo sapiens tryptophan 2,3-dioxygenase (TDO2), mRNA.
TELO2	2.39	Homo sapiens TEL2, telomere maintenance 2, homolog (S. cerevisiae) (TELO2), mRNA.
ANGPTL4	2.27	Homo sapiens angiopoietin-like 4 (ANGPTL4), transcript variant 1, mRNA.
MAP2	2.21	Homo sapiens microtubule-associated protein 2 (MAP2), transcript variant 1, mRNA.
GPR1	2.13	Homo sapiens G protein-coupled receptor 1 (GPR1), transcript variant 2, mRNA.
FAM167A	2.13	Homo sapiens family with sequence similarity 167, member A (FAM167A), mRNA.
RPS7	2.13	Homo sapiens ribosomal protein S7 (RPS7), mRNA.
TSPAN13	2.13	Homo sapiens tetraspanin 13 (TSPAN13), mRNA.
SYT7	2.12	Homo sapiens synaptotagmin VII (SYT7), mRNA.
ECE2	2.11	Homo sapiens endothelin converting enzyme 2 (ECE2), transcript variant 3, mRNA.
C8ORF13	2.07	Homo sapiens chromosome 8 open reading frame 13 (C8orf13), mRNA.
RPS7	2.06	Homo sapiens ribosomal protein S7 (RPS7), mRNA.
DHRS7	2.05	Homo sapiens dehydrogenase/reductase (SDR family) member 7 (DHRS7), mRNA.

ST6GALNAC3	2.05	Homo sapiens ST6 (alpha-N-acetyl-neuraminyl-2,3-beta-galactosyl-1, 3)-N-acetylgalactosaminide alpha-2, 6-sialyltransferase 3 (ST6GALNAC3), mRNA.
DIAPH3	-2.05	Homo sapiens diaphanous homolog 3 (Drosophila) (DIAPH3), transcript variant 1, mRNA.
LOC649143	-2.05	PREDICTED: Homo sapiens similar to HLA class II histocompatibility antigen, DRB1-9 beta chain precursor (MHC class I antigen DRB1*9) (DR-9) (DR9), transcript variant 2 (LOC649143), mRNA.
FOXM1	-2.06	Homo sapiens forkhead box M1 (FOXM1), transcript variant 2, mRNA.
CCL3L3	-2.06	Homo sapiens chemokine (C-C motif) ligand 3-like 3 (CCL3L3), mRNA.
ELF3	-2.06	Homo sapiens E74-like factor 3 (ets domain transcription factor, epithelial-specific) (ELF3), mRNA.
ADD3	-2.06	Homo sapiens adducin 3 (gamma) (ADD3), transcript variant 3, mRNA.
HLA-DRB6	-2.06	Homo sapiens major histocompatibility complex, class II, DR beta 6 (pseudogene) (HLA-DRB6), non-coding RNA.
CKAP2L	-2.07	Homo sapiens cytoskeleton associated protein 2-like (CKAP2L), mRNA.
CALD1	-2.07	Homo sapiens caldesmon 1 (CALD1), transcript variant 5, mRNA.
FLJ21986	-2.07	Homo sapiens hypothetical protein FLJ21986 (FLJ21986), mRNA.
ADD3	-2.07	Homo sapiens adducin 3 (gamma) (ADD3), transcript variant 3, mRNA.
NNMT	-2.08	Homo sapiens nicotinamide N-methyltransferase (NNMT), mRNA.
ENPEP	-2.08	Homo sapiens glutamyl aminopeptidase (aminopeptidase A) (ENPEP), mRNA.
NUF2	-2.09	Homo sapiens NUF2, NDC80 kinetochore complex component, homolog (S. cerevisiae) (NUF2), transcript variant 2, mRNA.
LYPD1	-2.09	Homo sapiens LY6/PLAUR domain containing 1 (LYPD1), transcript variant 1, mRNA.
CCNA2	-2.09	Homo sapiens cyclin A2 (CCNA2), mRNA.
ANKRD22	-2.09	Homo sapiens ankyrin repeat domain 22 (ANKRD22), mRNA.
P4HA2	-2.09	Homo sapiens prolyl 4-hydroxylase, alpha polypeptide II (P4HA2), transcript variant 2, mRNA.
COL4A2	-2.10	Homo sapiens collagen, type IV, alpha 2 (COL4A2), mRNA.
C10ORF58	-2.10	Homo sapiens chromosome 10 open reading frame 58 (C10orf58), transcript variant 1, mRNA.
DIAPH3	-2.11	Homo sapiens diaphanous homolog 3 (Drosophila) (DIAPH3), transcript variant 1, mRNA.
CHN1	-2.11	Homo sapiens chimerin (chimaerin) 1 (CHN1), transcript variant 2, mRNA.
FANCI	-2.11	Homo sapiens Fanconi anemia, complementation group I (FANCI), transcript variant 2, mRNA.
HJURP	-2.11	Homo sapiens Holliday junction recognition protein (HJURP), mRNA.
ACSL5	-2.11	Homo sapiens acyl-CoA synthetase long-chain family member 5 (ACSL5), transcript variant 2, mRNA.

HLA-DRB5	-2.12	Homo sapiens major histocompatibility complex, class II, DR beta 5 (HLA-DRB5), mRNA.
BNIP3L	-2.12	Homo sapiens BCL2/adenovirus E1B 19kDa interacting protein 3-like (BNIP3L), mRNA.
LIMK2	-2.12	Homo sapiens LIM domain kinase 2 (LIMK2), transcript variant 1, mRNA.
FBXO32	-2.13	Homo sapiens F-box protein 32 (FBXO32), transcript variant 2, mRNA.
CCL11	-2.14	Homo sapiens chemokine (C-C motif) ligand 11 (CCL11), mRNA.
TMEM45A	-2.15	Homo sapiens transmembrane protein 45A (TMEM45A), mRNA.
XIRP1	-2.17	Homo sapiens xin actin-binding repeat containing 1 (XIRP1), mRNA.
KIF23	-2.17	Homo sapiens kinesin family member 23 (KIF23), transcript variant 2, mRNA.
MAP1LC3A	-2.17	Homo sapiens microtubule-associated protein 1 light chain 3 alpha (MAP1LC3A), transcript variant 2, mRNA.
ENO2	-2.18	Homo sapiens enolase 2 (gamma, neuronal) (ENO2), mRNA.
FRMD4A	-2.18	Homo sapiens FERM domain containing 4A (FRMD4A), mRNA.
CXCL6	-2.19	Homo sapiens chemokine (C-X-C motif) ligand 6 (granulocyte chemotactic protein 2) (CXCL6), mRNA.
ABCA6	-2.19	Homo sapiens ATP-binding cassette, sub-family A (ABC1), member 6 (ABCA6), mRNA.
C6ORF173	-2.19	Homo sapiens chromosome 6 open reading frame 173 (C6orf173), mRNA.
ARHGEF3	-2.20	Homo sapiens Rho guanine nucleotide exchange factor (GEF) 3 (ARHGEF3), mRNA.
FABP3	-2.20	Homo sapiens fatty acid binding protein 3, muscle and heart (mammary-derived growth inhibitor) (FABP3), mRNA.
AQP9	-2.20	Homo sapiens aquaporin 9 (AQP9), mRNA.
TEX11	-2.20	Homo sapiens testis expressed 11 (TEX11), transcript variant 1, mRNA.
CDC45L	-2.20	Homo sapiens CDC45 cell division cycle 45-like (S. cerevisiae) (CDC45L), mRNA.
IGFBP5	-2.22	Homo sapiens insulin-like growth factor binding protein 5 (IGFBP5), mRNA.
NHS	-2.22	Homo sapiens Nance-Horan syndrome (congenital cataracts and dental anomalies) (NHS), transcript variant 1, mRNA.
ACSL5	-2.22	Homo sapiens acyl-CoA synthetase long-chain family member 5 (ACSL5), transcript variant 1, mRNA.
NDP	-2.22	Homo sapiens Norrie disease (pseudoglioma) (NDP), mRNA.
LOC100133923	-2.22	PREDICTED: Homo sapiens hypothetical protein LOC100133923 (LOC100133923), mRNA.
KIF2C	-2.23	Homo sapiens kinesin family member 2C (KIF2C), mRNA.
RARRES1	-2.23	Homo sapiens retinoic acid receptor responder (tazarotene induced) 1 (RARRES1), transcript variant 1, mRNA.
MYLK	-2.23	Homo sapiens myosin light chain kinase (MYLK), transcript variant 8, mRNA.

SIRPA	-2.24	Homo sapiens signal-regulatory protein alpha (SIRPA), transcript variant 3, mRNA.
ROR2	-2.24	Homo sapiens receptor tyrosine kinase-like orphan receptor 2 (ROR2), mRNA.
PIM1	-2.26	Homo sapiens pim-1 oncogene (PIM1), mRNA.
KIF11	-2.26	Homo sapiens kinesin family member 11 (KIF11), mRNA.
GRAMD3	-2.26	Homo sapiens GRAM domain containing 3 (GRAMD3), mRNA.
ZWINT	-2.26	Homo sapiens ZW10 interactor (ZWINT), transcript variant 3, mRNA.
INSIG2	-2.26	Homo sapiens insulin induced gene 2 (INSIG2), mRNA.
NUSAP1	-2.27	Homo sapiens nucleolar and spindle associated protein 1 (NUSAP1), transcript variant 2, mRNA.
PIK3IP1	-2.27	Homo sapiens phosphoinositide-3-kinase interacting protein 1 (PIK3IP1), mRNA.
CDCA5	-2.27	Homo sapiens cell division cycle associated 5 (CDCA5), mRNA.
NCCRP1	-2.29	Homo sapiens non-specific cytotoxic cell receptor protein 1 homolog (zebrafish) (NCCRP1), mRNA.
PLAT	-2.29	Homo sapiens plasminogen activator, tissue (PLAT), transcript variant 1, mRNA.
CXCL9	-2.29	Homo sapiens chemokine (C-X-C motif) ligand 9 (CXCL9), mRNA.
HNMT	-2.30	Homo sapiens histamine N-methyltransferase (HNMT), transcript variant 2, mRNA.
LOC100131093	-2.30	PREDICTED: Homo sapiens misc_RNA (LOC100131093), miscRNA.
TACC3	-2.30	Homo sapiens transforming, acidic coiled-coil containing protein 3 (TACC3), mRNA.
DLGAP5	-2.32	Homo sapiens discs, large (Drosophila) homolog-associated protein 5 (DLGAP5), mRNA.
JAM2	-2.32	Homo sapiens junctional adhesion molecule 2 (JAM2), mRNA.
TPX2	-2.33	Homo sapiens TPX2, microtubule-associated, homolog (Xenopus laevis) (TPX2), mRNA.
PSTPIP2	-2.34	Homo sapiens proline-serine-threonine phosphatase interacting protein 2 (PSTPIP2), mRNA.
ASF1B	-2.36	Homo sapiens ASF1 anti-silencing function 1 homolog B (S. cerevisiae) (ASF1B), mRNA.
HECW2	-2.37	Homo sapiens HECT, C2 and WW domain containing E3 ubiquitin protein ligase 2 (HECW2), mRNA.
CLDN7	-2.37	Homo sapiens claudin 7 (CLDN7), mRNA.
G0S2	-2.38	Homo sapiens G0/G1switch 2 (G0S2), mRNA.
CEACAM1	-2.38	Homo sapiens carcinoembryonic antigen-related cell adhesion molecule 1 (biliary glycoprotein) (CEACAM1), transcript variant 2, mRNA.
HMMR	-2.39	Homo sapiens hyaluronan-mediated motility receptor (RHAMM) (HMMR), transcript variant 2, mRNA.
FAM20A	-2.39	Homo sapiens family with sequence similarity 20, member A (FAM20A), mRNA.

CCNB2	-2.40	Homo sapiens cyclin B2 (CCNB2), mRNA.
HLA-F	-2.40	Homo sapiens major histocompatibility complex, class I, F (HLA-F), transcript variant 1, mRNA.
NOD2	-2.40	Homo sapiens nucleotide-binding oligomerization domain containing 2 (NOD2), mRNA.
RARRES3	-2.44	Homo sapiens retinoic acid receptor responder (tazarotene induced) 3 (RARRES3), mRNA.
STEAP4	-2.46	Homo sapiens STEAP family member 4 (STEAP4), mRNA.
ASCL2	-2.47	Homo sapiens achaete-scute complex homolog 2 (Drosophila) (ASCL2), mRNA.
AK3L1	-2.50	Homo sapiens adenylate kinase 3-like 1 (AK3L1), nuclear gene encoding mitochondrial protein, transcript variant 7, mRNA.
MT3	-2.51	Homo sapiens metallothionein 3 (MT3), mRNA.
ACAT2	-2.51	Homo sapiens acetyl-Coenzyme A acetyltransferase 2 (ACAT2), mRNA.
CEP55	-2.51	Homo sapiens centrosomal protein 55kDa (CEP55), mRNA.
ASPM	-2.52	Homo sapiens asp (abnormal spindle) homolog, microcephaly associated (Drosophila) (ASPM), mRNA.
AK3L1	-2.52	Homo sapiens adenylate kinase 3-like 1 (AK3L1), nuclear gene encoding mitochondrial protein, transcript variant 6, mRNA.
CARHSP1	-2.53	Homo sapiens calcium regulated heat stable protein 1, 24kDa (CARHSP1), transcript variant 2, mRNA.
MT1F	-2.53	Homo sapiens metallothionein 1F (MT1F), mRNA.
CDC2	-2.55	Homo sapiens cell division cycle 2, G1 to S and G2 to M (CDC2), transcript variant 1, mRNA.
IL1A	-2.55	Homo sapiens interleukin 1, alpha (IL1A), mRNA.
IL4I1	-2.57	Homo sapiens interleukin 4 induced 1 (IL4I1), transcript variant 2, mRNA.
TYMS	-2.57	Homo sapiens thymidylate synthetase (TYMS), mRNA.
CDKN3	-2.58	Homo sapiens cyclin-dependent kinase inhibitor 3 (CDK2-associated dual specificity phosphatase) (CDKN3), mRNA.
KIF4A	-2.59	Homo sapiens kinesin family member 4A (KIF4A), mRNA.
CDCA3	-2.59	Homo sapiens cell division cycle associated 3 (CDCA3), mRNA.
ALDOC	-2.59	Homo sapiens aldolase C, fructose-bisphosphate (ALDOC), mRNA.
ADAMDEC1	-2.59	Homo sapiens ADAM-like, decysin 1 (ADAMDEC1), mRNA.
KIFC1	-2.62	Homo sapiens kinesin family member C1 (KIFC1), mRNA.
CD38	-2.63	Homo sapiens CD38 molecule (CD38), mRNA.
NDC80	-2.64	Homo sapiens NDC80 homolog, kinetochore complex component (S. cerevisiae) (NDC80), mRNA.

MELK	-2.64	Homo sapiens maternal embryonic leucine zipper kinase (MELK), mRNA.
HLA-DRB6	-2.64	Homo sapiens major histocompatibility complex, class II, DR beta 6 (pseudogene) (HLA-DRB6), non-coding RNA.
MMP9	-2.65	Homo sapiens matrix metallopeptidase 9 (gelatinase B, 92kDa gelatinase, 92kDa type IV collagenase) (MMP9), mRNA.
TP53INP2	-2.66	Homo sapiens tumor protein p53 inducible nuclear protein 2 (TP53INP2), mRNA.
BIRC5	-2.66	Homo sapiens baculoviral IAP repeat-containing 5 (BIRC5), transcript variant 1, mRNA.
SHRM	-2.70	Homo sapiens shroom (SHRM), mRNA.
HLA-DRB1	-2.70	Homo sapiens major histocompatibility complex, class II, DR beta 1 (HLA-DRB1), mRNA.
RRM2	-2.70	Homo sapiens ribonucleotide reductase M2 polypeptide (RRM2), mRNA.
SRGN	-2.74	Homo sapiens serglycin (SRGN), mRNA.
MT1JP	-2.75	Homo sapiens metallothionein 1J (pseudogene) (MT1JP), mRNA.
AK3L1	-2.76	Homo sapiens adenylate kinase 3-like 1 (AK3L1), nuclear gene encoding mitochondrial protein, transcript variant 7, mRNA.
SLC39A8	-2.77	Homo sapiens solute carrier family 39 (zinc transporter), member 8 (SLC39A8), transcript variant 1, mRNA.
RARRES1	-2.77	Homo sapiens retinoic acid receptor responder (tazarotene induced) 1 (RARRES1), transcript variant 2, mRNA.
TK1	-2.79	Homo sapiens thymidine kinase 1, soluble (TK1), mRNA.
PBK	-2.79	Homo sapiens PDZ binding kinase (PBK), mRNA.
JUP	-2.81	Homo sapiens junction plakoglobin (JUP), transcript variant 1, mRNA.
APOBEC3B	-2.84	Homo sapiens apolipoprotein B mRNA editing enzyme, catalytic polypeptide-like 3B (APOBEC3B), mRNA.
HMMR	-2.85	Homo sapiens hyaluronan-mediated motility receptor (RHAMM) (HMMR), transcript variant 1, mRNA.
DLGAP5	-2.91	Homo sapiens discs, large (Drosophila) homolog-associated protein 5 (DLGAP5), mRNA.
SCARA3	-2.93	Homo sapiens scavenger receptor class A, member 3 (SCARA3), transcript variant 1, mRNA.
C9ORF135	-2.96	Homo sapiens chromosome 9 open reading frame 135 (C9orf135), mRNA.
CYB5A	-2.97	Homo sapiens cytochrome b5 type A (microsomal) (CYB5A), transcript variant 2, mRNA.
RASD1	-2.98	Homo sapiens RAS, dexamethasone-induced 1 (RASD1), mRNA.
ANLN	-2.98	Homo sapiens anillin, actin binding protein (ANLN), mRNA.
KIF11	-2.99	Homo sapiens kinesin family member 11 (KIF11), mRNA.

SCARA3	-3.02	Homo sapiens scavenger receptor class A, member 3 (SCARA3), transcript variant 2, mRNA.
IL32	-3.03	Homo sapiens interleukin 32 (IL32), transcript variant 4, mRNA.
HLA-DPA1	-3.04	Homo sapiens major histocompatibility complex, class II, DP alpha 1 (HLA-DPA1), mRNA.
KIAA0101	-3.05	Homo sapiens KIAA0101 (KIAA0101), transcript variant 1, mRNA.
CDC2	-3.07	Homo sapiens cell division cycle 2, G1 to S and G2 to M (CDC2), transcript variant 1, mRNA.
TNFSF10	-3.16	Homo sapiens tumor necrosis factor (ligand) superfamily, member 10 (TNFSF10), mRNA.
SRGN	-3.21	Homo sapiens serglycin (SRGN), mRNA.
SEPT4	-3.21	Homo sapiens septin 4 (SEPT4), transcript variant 1, mRNA.
MT1H	-3.22	Homo sapiens metallothionein 1H (MT1H), mRNA.
MUC1	-3.28	Homo sapiens mucin 1, cell surface associated (MUC1), transcript variant 6, mRNA.
SEPT4	-3.29	Homo sapiens septin 4 (SEPT4), transcript variant 3, mRNA.
HS.10862	-3.32	Homo sapiens cDNA: FLJ23313 fis, clone HEP11919
SLC26A4	-3.33	Homo sapiens solute carrier family 26, member 4 (SLC26A4), mRNA.
SLC39A8	-3.35	Homo sapiens solute carrier family 39 (zinc transporter), member 8 (SLC39A8), transcript variant 1, mRNA.
IGFBP7	-3.35	Homo sapiens insulin-like growth factor binding protein 7 (IGFBP7), mRNA.
AURKB	-3.37	Homo sapiens aurora kinase B (AURKB), mRNA.
HLA-DRB4	-3.37	Homo sapiens major histocompatibility complex, class II, DR beta 4 (HLA-DRB4), mRNA.
NUSAP1	-3.38	Homo sapiens nucleolar and spindle associated protein 1 (NUSAP1), transcript variant 2, mRNA.
SAA1	-3.39	Homo sapiens serum amyloid A1 (SAA1), transcript variant 2, mRNA.
NCAPG	-3.47	Homo sapiens non-SMC condensin I complex, subunit G (NCAPG), mRNA.
UBE2C	-3.54	Homo sapiens ubiquitin-conjugating enzyme E2C (UBE2C), transcript variant 3, mRNA.
CYB5A	-3.55	Homo sapiens cytochrome b5 type A (microsomal) (CYB5A), transcript variant 2, mRNA.
HLA-DRA	-3.58	Homo sapiens major histocompatibility complex, class II, DR alpha (HLA-DRA), mRNA.
UBE2C	-3.60	Homo sapiens ubiquitin-conjugating enzyme E2C (UBE2C), transcript variant 6, mRNA.
HIST1H4C	-3.63	Homo sapiens histone cluster 1, H4c (HIST1H4C), mRNA.

PRC1	-3.66	Homo sapiens protein regulator of cytokinesis 1 (PRC1), transcript variant 2, mRNA.
TOP2A	-3.71	Homo sapiens topoisomerase (DNA) II alpha 170kDa (TOP2A), mRNA.
PALLD	-3.94	Homo sapiens palladin, cytoskeletal associated protein (PALLD), transcript variant 2, mRNA.
HAS3	-3.96	Homo sapiens hyaluronan synthase 3 (HAS3), transcript variant 1, mRNA.
VCAM1	-4.27	Homo sapiens vascular cell adhesion molecule 1 (VCAM1), transcript variant 1, mRNA.
LOC730415	-4.42	PREDICTED: Homo sapiens hypothetical LOC730415, transcript variant 2 (LOC730415), mRNA.
VCAM1	-4.67	Homo sapiens vascular cell adhesion molecule 1 (VCAM1), transcript variant 1, mRNA.
HLA-DRA	-4.70	Homo sapiens major histocompatibility complex, class II, DR alpha (HLA-DRA), mRNA.
METTL7A	-4.71	Homo sapiens methyltransferase like 7A (METTL7A), mRNA.
CFB	-4.83	Homo sapiens complement factor B (CFB), mRNA.
CX3CL1	-5.09	Homo sapiens chemokine (C-X3-C motif) ligand 1 (CX3CL1), mRNA.
SEPT4	-5.21	Homo sapiens septin 4 (SEPT4), transcript variant 2, mRNA.
LIPG	-5.24	Homo sapiens lipase, endothelial (LIPG), mRNA.
UBD	-5.80	Homo sapiens ubiquitin D (UBD), mRNA.
HSD11B1	-5.88	Homo sapiens hydroxysteroid (11-beta) dehydrogenase 1 (HSD11B1), transcript variant 2, mRNA.
CD74	-6.12	Homo sapiens CD74 molecule, major histocompatibility complex, class II invariant chain (CD74), transcript variant 2, mRNA.
SLC2A5	-6.54	Homo sapiens solute carrier family 2 (facilitated glucose/fructose transporter), member 5 (SLC2A5), mRNA.
HSD11B1	-6.77	Homo sapiens hydroxysteroid (11-beta) dehydrogenase 1 (HSD11B1), transcript variant 2, mRNA.
CCL5	-7.10	Homo sapiens chemokine (C-C motif) ligand 5 (CCL5), mRNA.
MYH11	-7.65	Homo sapiens myosin, heavy chain 11, smooth muscle (MYH11), transcript variant SM1A, mRNA.
HSD11B1	-7.87	Homo sapiens hydroxysteroid (11-beta) dehydrogenase 1 (HSD11B1), transcript variant 1, mRNA.
CD74	-8.00	Homo sapiens CD74 molecule, major histocompatibility complex, class II invariant chain (CD74), transcript variant 1, mRNA.
CCL5	-10.74	Homo sapiens chemokine (C-C motif) ligand 5 (CCL5), mRNA.

Further analysis showed that the bioactivity of theEOB significantly overlapped with many canonical pathways from the literature-validated database (Figure 2). Many of these signaling pathways are closely related to the inflammatory, immunomodulatory, and wound healing processes, as well as cancer signaling in human cells. For

example, the top two matched pathways werehepatic fibrosis activation and antigen presentation. The robust inhibitory effect of the EOB on these four pathways and genes support its inflammatory and immunomodulatory properties (Tables S3-S6). The observation that the EOB significantly affected pathways related to DNA damage response and cell cycle control (e.g., mitotic roles of the polo-like kinase, cyclins, and cell cycle regulation) suggests thatthe EOB may have an effect oncancer biology and signaling (Figure 2).

Table S3. *Top 20 genes regulated by EOB in the Hepatic Fibrosis/Hepatic Stellate Cell Activation canonical path way. Fold change over vehicle is shown as a log2 ratio.*

Gene Symbol	Entrez Gene Name	Illumina Probe ID	Location	Protein Type	Entrez Gene ID for Human	Fold Change Over Vehicle
TGFB3	transforming growth factor, beta 3	ILMN_1687652	Extracellular Space	growth factor	7043	1.666
MYL5	myosin, light chain 5, regulatory	ILMN_2203588	Cytoplasm	other	4636	1.644
TIMP2	TIMP metallopeptidase inhibitor 2	ILMN_1721876	Extracellular Space	other	7077	-1.608
A2M	alpha-2-macroglobulin	ILMN_1745607	Extracellular Space	transporter	2	-1.650
COL6A3	collagen, type VI, alpha 3	ILMN_2307861	Extracellular Space	other	1293	-1.677
CD40	CD40 molecule, TNF receptor superfamily member 5	ILMN_1779257	Plasma Membrane	transmembrane receptor	958	-1.715
COL18A1	collagen, type XVIII, alpha 1	ILMN_1806733	Extracellular Space	other	80781	-1.840
EDNRA	endothelin receptor type A	ILMN_1796629	Plasma Membrane	transmembrane receptor	1909	-1.883
EDNRB	endothelin receptor type B	ILMN_1751904	Plasma Membrane	G-protein coupled receptor	1910	-1.909
COL1A2	collagen, type I, alpha 2	ILMN_1785272	Extracellular Space	other	1278	-1.992
IGFBP3	insulin-like growth factor binding protein 3	ILMN_1746085	Extracellular Space	other	3486	-2.035
MYH10	myosin, heavy chain 10, non-muscle	ILMN_1815154	Cytoplasm	other	4628	-2.036
COL4A2	collagen, type IV, alpha 2	ILMN_1724994	Extracellular Space	other	1284	-2.102
IGFBP5	insulin-like growth factor binding protein 5	ILMN_2132982	Extracellular Space	other	3488	-2.216
CXCL9	chemokine (C-X-C motif) ligand 9	ILMN_1745356	Extracellular Space	cytokine	4283	-2.292
IL1A	interleukin 1, alpha	ILMN_1658483	Extracellular Space	cytokine	3552	-2.550
MMP9	matrix metallopeptidase 9	ILMN_1796316	Extracellular Space	peptidase	4318	-2.653
VCAM1	vascular cell adhesion molecule 1	ILMN_2307903	Plasma Membrane	transmembrane receptor	7412	-4.670
MYH11	myosin, heavy chain 11, smooth muscle	ILMN_1660086	Cytoplasm	other	4629	-7.654
CCL5	chemokine (C-C motif) ligand 5	ILMN_1773352	Extracellular Space	cytokine	6352	-10.744

Table S4. *Top 20 genes regulated by EOB in the Antigen Presentation canonical pathway. Fold change over vehicle is shown as a log2 ratio.*

Gene Symbol	Entrez Gene Name	Illumina Probe ID	Location	Protein Type	Entrez Gene ID for Human	Fold Change Over Vehicle
PSMB8	proteasome (prosome, macropain) subunit, beta type, 8	ILMN_2284794	Cytoplasm	peptidase	5696	-1.278
IFNG	interferon, gamma	ILMN_2207291	Extracellular Space	cytokine	3458	-1.305
HLA-C	major histocompatibility complex, class I, C	ILMN_1721113	Plasma Membrane	other	3107	-1.449
HLA-DQA1	major histocompatibility complex, class II, DQ alpha 1	ILMN_1808405	Plasma Membrane	transmembrane receptor	3117	-1.485
PSMB9	proteasome (prosome, macropain) subunit, beta type, 9	ILMN_2376108	Cytoplasm	peptidase	5698	-1.491
HLA-DOA	major histocompatibility complex, class II, DO alpha	ILMN_1659075	Plasma Membrane	transmembrane receptor	3111	-1.498
HLA-G	major histocompatibility complex, class I, G	ILMN_1656670	Plasma Membrane	other	3135	-1.598
HLA-B	major histocompatibility complex, class I, B	ILMN_1778401	Plasma Membrane	transmembrane receptor	3106	-1.612
HLA-A	major histocompatibility complex, class I, A	ILMN_2165753	Plasma Membrane	other	3105	-1.681
MR1	major histocompatibility complex, class I-related	ILMN_2167416	Plasma Membrane	transmembrane receptor	3140	-1.697
TAPBP	TAP binding protein (tapasin)	ILMN_1742450	Cytoplasm	transporter	6892	-1.722
HLA-DMA	major histocompatibility complex, class II, DM alpha	ILMN_1695311	Plasma Membrane	transmembrane receptor	3108	-2.036
HLA-DMB	major histocompatibility complex, class II, DM beta	ILMN_1761733	Plasma Membrane	transmembrane receptor	3109	-2.045
HLA-DRB5	major histocompatibility complex, class II, DR beta 5	ILMN_1697499	Plasma Membrane	transmembrane receptor	3127	-2.116
HLA-F	major histocompatibility complex, class I, F	ILMN_1762861	Plasma Membrane	transmembrane receptor	3134	-2.402
HLA-DPA1	major histocompatibility complex, class II, DP alpha 1	ILMN_1772218	Plasma Membrane	transmembrane receptor	3113	-3.037
HLA-DRB4	major histocompatibility complex, class II, DR beta 4	ILMN_1752592	Plasma Membrane	transmembrane receptor	3126	-3.370
HLA-DRB1	major histocompatibility complex, class II, DR beta 1	ILMN_3228688	Plasma Membrane	transmembrane receptor	3123	-4.415
HLA-DRA	major histocompatibility complex, class II, DR alpha	ILMN_2157441	Plasma Membrane	transmembrane receptor	3122	-4.696
CD74	CD74 molecule, major histocompatibility complex, class II invariant chain	ILMN_1736567	Plasma Membrane	transmembrane receptor	972	-7.999

Table S5. *Top 20 genes regulated by EOB in the Mitotic Roles of Polo-Like Kinase canonical pathway. Fold change over vehicle is shown as a log2 ratio.*

Gene Symbol	Entrez Gene Name	Illumina Probe ID	Location	Protein Type	Entrez Gene ID for Human	Fold Change Over Vehicle
FZR1	fizzy/cell division cycle 20 related 1 (Drosophila)	ILMN_3306993	Nucleus	kinase	51343	1.389
PPP2R2A	protein phosphatase 2, regulatory subunit B, alpha	ILMN_1788961	Cytoplasm	phosphatase	5520	1.330
RAD21	RAD21 homolog (S. pombe)	ILMN_1748578	Nucleus	other	5885	-1.352
CCNB3	cyclin B3	ILMN_1705757	Nucleus	other	85417	-1.361
PPP2R4	protein phosphatase 2A activator, regulatory subunit 4	ILMN_1658951	Cytoplasm	phosphatase	5524	-1.371
PTTG1	pituitary tumor-transforming 1	ILMN_2042771	Nucleus	transcription regulator	9232	-1.407
PPP2R3B	protein phosphatase 2, regulatory subunit B", beta	ILMN_1712257	Nucleus	phosphatase	28227	-1.411
PKMYT1	protein kinase, membrane associated tyrosine/threonine 1	ILMN_2401436	Cytoplasm	kinase	9088	-1.414
WEE1	WEE1 G2 checkpoint kinase	ILMN_1778561	Nucleus	kinase	7465	-1.470
PLK1	polo-like kinase 1	ILMN_1736176	Nucleus	kinase	5347	-1.531
CCNB1	cyclin B1	ILMN_1712803	Cytoplasm	kinase	891	-1.621
CDC20	cell division cycle 20	ILMN_1663390	Nucleus	other	991	-1.778
FBXO5	F-box protein 5	ILMN_1710676	Nucleus	enzyme	26271	-1.785
PLK4	polo-like kinase 4	ILMN_1789123	Cytoplasm	kinase	10733	-1.849
CDC25C	cell division cycle 25C	ILMN_1725260	Nucleus	phosphatase	995	-1.905
KIF23	kinesin family member 23	ILMN_1811472	Cytoplasm	other	9493	-2.166
CCNB2	cyclin B2	ILMN_1801939	Cytoplasm	other	9133	-2.398
KIF11	kinesin family member 11	ILMN_2143155	Nucleus	other	3832	-2.987
CDK1	cyclin-dependent kinase 1	ILMN_1747911	Nucleus	kinase	983	-3.065
PRC1	protein regulator of cytokinesis 1	ILMN_1728934	Nucleus	other	9055	-3.664

Table S6. *Top 20 genes regulated by EOB in the Cyclins and Cell Cycle Regulation canonical pathway. Fold change over vehicle is shown as a log2 ratio.*

Gene Symbol	Entrez Gene Name	Illumina Probe ID	Location	Protein Type	Entrez Gene ID for Human	Fold Change Over Vehicle
E2F5	E2F transcription factor 5, p130-binding	ILMN_1782551	Nucleus	transcription regulator	1875	1.901
TGFB3	transforming growth factor, beta 3	ILMN_1687652	Extracellular Space	growth factor	7043	1.666
PA2G4	proliferation-associated 2G4, 38kDa	ILMN_1728984	Nucleus	transcription regulator	5036	1.395
CDKN2C	cyclin-dependent kinase inhibitor 2C (p18, inhibits CDK4)	ILMN_2359332	Nucleus	transcription regulator	1031	1.387
HDAC2	histone deacetylase 2	ILMN_1767747	Nucleus	transcription regulator	3066	1.337
PPP2R2A	protein phosphatase 2, regulatory subunit B, alpha	ILMN_1788961	Cytoplasm	phosphatase	5520	1.330
CCNB3	cyclin B3	ILMN_1705757	Nucleus	other	85417	-1.361
CDK2	cyclin-dependent kinase 2	ILMN_1665559	Nucleus	kinase	1017	-1.368
PPP2R4	protein phosphatase 2A activator, regulatory subunit 4	ILMN_1658951	Cytoplasm	phosphatase	5524	-1.371
PPP2R3B	protein phosphatase 2, regulatory subunit B", beta	ILMN_1712257	Nucleus	phosphatase	28227	-1.411
RB1	retinoblastoma 1	ILMN_1696591	Nucleus	transcription regulator	5925	-1.411
E2F2	E2F transcription factor 2	ILMN_1777233	Nucleus	transcription regulator	1870	-1.444
WEE1	WEE1 G2 checkpoint kinase	ILMN_1778561	Nucleus	kinase	7465	-1.470
CDKN1B	cyclin-dependent kinase inhibitor 1B (p27, Kip1)	ILMN_2196347	Nucleus	kinase	1027	-1.479
CCNB1	cyclin B1	ILMN_1712803	Cytoplasm	kinase	891	-1.621
CDKN2B	cyclin-dependent kinase inhibitor 2B (p15, inhibits CDK4)	ILMN_2376723	Nucleus	transcription regulator	1030	-1.766
CCNE2	cyclin E2	ILMN_2412384	Nucleus	other	9134	-1.827
CCNA2	cyclin A2	ILMN_1786125	Nucleus	other	890	-2.088
CCNB2	cyclin B2	ILMN_1801939	Cytoplasm	other	9133	-2.398
CDK1	cyclin-dependent kinase 1	ILMN_1747911	Nucleus	kinase	983	-3.065

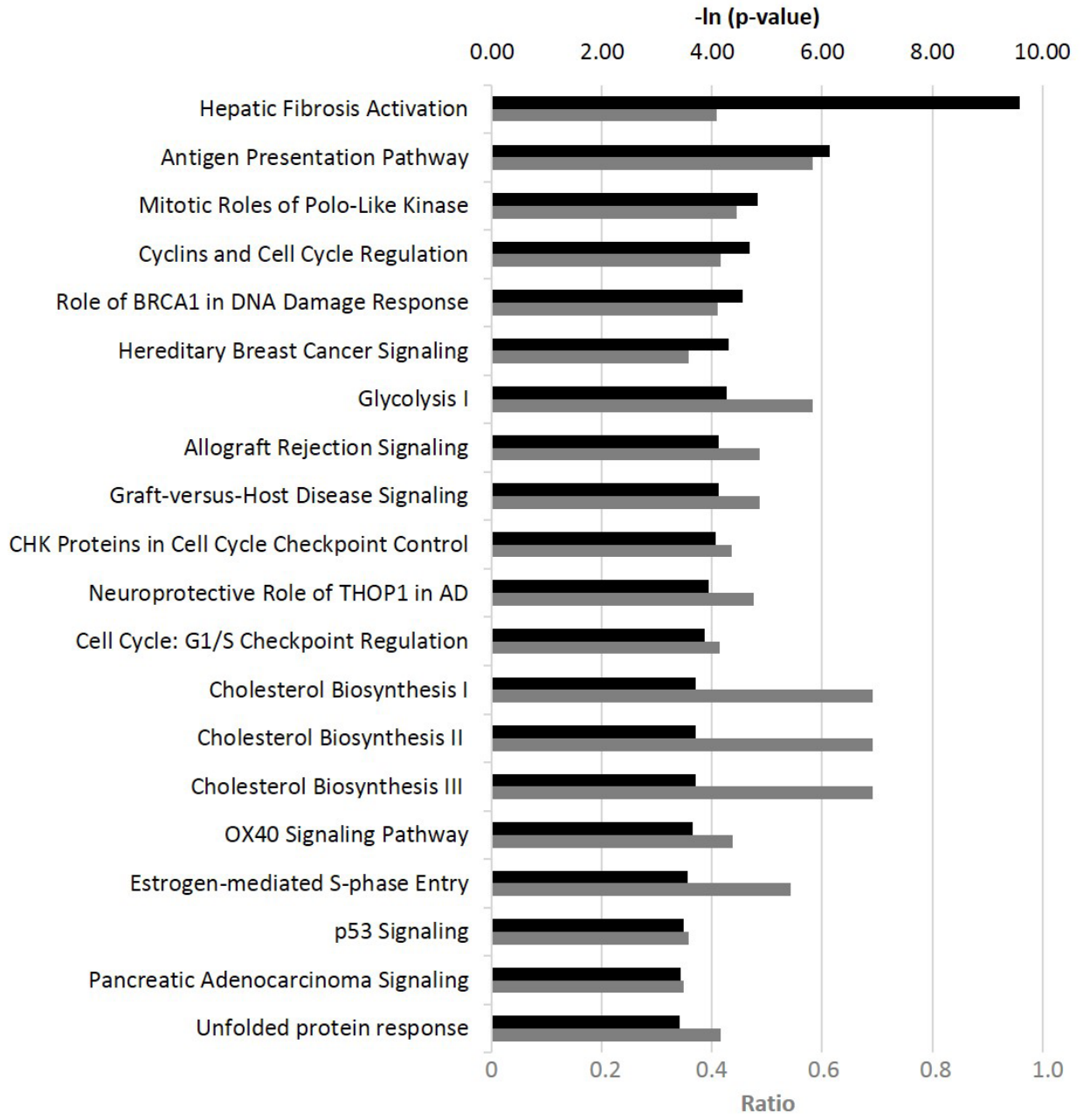

Fig2. *Top 20 canonical pathways matching the bioactivity profile of the essential oil blend (EOB, 0.0033% v/v) in gene expression in an HDF3CGF system, produced using Ingenuity Pathway Analysis (IPA). Each p-value was calculated using the right-tailed Fisher's exact test. The p-value measures the likelihood that the observed association between a specific pathway and the dataset is due to random chance. Pathways with smaller p-values (bigger - ln [p-values], indicated by the black bars) matched the bioactivity of the EOB more significantly than those with higher values did. A ratio, indicated by each gray bar, was calculated by taking the number of genes from the EOB dataset that participate in a canonical pathway and dividing it by the total number of genes in that pathway. BRCA1, human breast cancer gene 1; THOP1, thimetoligopeptidase; AD, Alzheimer's disease; OX40 (TNFRSF4), tumor necrosis factor receptor superfamily, member 4; p53, tumor suppressor protein 53*

These results are also consistent with findings of other research studies on the biological activity of the primary chemical constituents of the EOB. For example, limonene inhibited the expression of a number of inflammatory genes in an osteoarthritis model (Rufino et al., 2015) and α-pinene affected immunomodulatory genes in a mouse model of allergic rhinitis (Nam et al., 2014). Eugenol, the third most abundant constituent in the EOB, is known for its anti-cancer and anti-inflammatory properties in various cell types. It has been shown to upregulate genes in the base excision repair pathway (Ghosh et al., 2005) while downregulating inflammatory cytokines (Pal et al., 2010) and antiapoptotic genes (Kaur et al., 2010).

This study provides important data on the biological activity of an EOB in cytokine-stimulated human dermal fibroblasts. The data suggest that the EOB may modulate inflammatory and immune responses, tissue remodeling, and cancer signaling processes in a manner unique to any individualoil studied previously. Further research is needed to elucidate the biological and physiological mechanisms of action of the EOB and any synergistic or antagonistic interactions between the compounds contained therein.

Conclusions

To the best of our knowledge, this is the first study to analyze the effect of an EOB on genome-wide gene expression in human skin cells. The EOBsignificantly modulated mRNA levelsof genes involved in a variety of important signaling pathways including inflammation, immune function, wound healing, cell cycle regulation, and DNA damage repair. It's biological activity is unique to any pure essential oil studied previously. This study providesoriginal and important data onthemodulation ofgenome-wide gene expression in validated human cell cultures by an essential oil blend.Finally, theseresults suggest that this EOB maypossess the potential to modulate inflammatory and immune responses in skin cells, giving it practical applications in the fields of dermatology and medicine in general.

Acknowledgment

This study was funded by dōTERRA (Pleasant Grove, UT, USA) and conducted at DiscoverX (Fremont, CA, USA). Xuesheng Han, Ph.D. designed the study, analyzed the data, and wrote the paper. Tyler Bahr, B. S. participated in writing the paper. The authors would like to acknowledge Carsten Smidt, Ph.D.; Tory Parker, Ph.D.; Cody Beaumont, Ph.D.; Jeff Dorsett, M.S.; and Nicole Stevens, M.S. for their support to the work.

Competing Interest

Xuesheng Han and Tyler Bahr are employees of dōTERRA,where the studied agent EOB was manufactured.

References

1. Barbosa-Morais, N. L., Dunning, M. J., Samarajiwa, S. A., Darot, J. F. J., Ritchie, M. E., Lynch, A. G., & Tavaré, S. (2010). A re-annotation pipeline for Illumina BeadArrays: improving the interpretation of gene expression data. *Nucleic Acids Research*, *38*(3), e17. https://doi.org/10.1093/nar/gkp942
2. Berg, E. L., Yang, J., Melrose, J., Nguyen, D., Privat, S., Rosler, E., &Ekins, S. (2010). Chemical target and pathway toxicity mechanisms defined in primary human cell systems. *Journal of Pharmacological and Toxicological Methods*, *61*(1), 3–15. https://doi.org/10.1016/j.vascn.2009.10.001
3. Bergamini, G., Bell, K., Shimamura, S., Werner, T., Cansfield, A., Müller, K., &Neubauer, G. (2012). A selective inhibitor reveals PI3Kγ dependence of T(H)17 cell differentiation. *Nature Chemical Biology*, *8*(6), 576–582. https://doi.org/10.1038/nchembio.957
4. Bolstad, B. M., Irizarry, R. A., Astrand, M., & Speed, T. P. (2003). A comparison of normalization methods for high density oligonucleotide array data based on variance and bias. *Bioinformatics (Oxford, England)*, *19*(2), 185–193.

5. Chaudhary, S. C., Siddiqui, M. S., Athar, M., & Alam, M. S. (2012). D-Limonene modulates inflammation, oxidative stress and Ras-ERK pathway to inhibit murine skin tumorigenesis. *Human & Experimental Toxicology*, *31*(8), 798–811. https://doi.org/10.1177/0960327111434948

6. Dunning, M. J., Smith, M. L., Ritchie, M. E., & Tavaré, S. (2007). beadarray: R classes and methods for Illumina bead-based data. *Bioinformatics (Oxford, England)*, *23*(16), 2183–2184. https://doi.org/10.1093/bioinformatics/btm311

7. Ghosh, R., Nadiminty, N., Fitzpatrick, J. E., Alworth, W. L., Slaga, T. J., & Kumar, A. P. (2004). Eugenol causes melanoma growth suppression through inhibition of E2F1 transcriptional activity. *Journal of Biological Chemistry*, 280(7), 5812-5819. doi:10.1074/jbc.m411429200

8. Han, X., & Parker, T. L. (2017a). Anti-inflammatory activity of Juniper (*Juniperus communis*) berry essential oil in human dermal fibroblasts. *Cogent Medicine*, *4*(1), 1306200. https://doi.org/10.1080/2331205X.2017.1306200

9. Han, X., & Parker, T. L. (2017b). Anti-inflammatory, tissue remodeling, immunomodulatory, and anticancer activities of oregano (*Origanum vulgare*) essential oil in a human skin disease model. *Biochimie Open*, 4, 73–77. https://doi.org/10.1016/j.biopen.2017.02.005

10. Han, X., & Parker, T. L. (2017c). Biological activities of frankincense essential oil in human dermal fibroblasts. *Biochimie Open*, 4, 31-35. doi:10.1016/j.biopen.2017.01.003

11. Han, X., & Parker, T. L. (2017d). Anti-inflammatory activity of clove (Eugenia caryophyllata) in human dermal fibroblasts. *Pharm Biol.*, 55(1), 1619-1622. https://doi.org/10.1080/13880209.2017.1314513

12. Han, X., Price, R., & Parker, T. L. (2017). An essential oil blend modulates important inflammation- and immune response-related biomarkers in human cell cocultures. *Cogent Medicine*, *0*(ja), 1302909. https://doi.org/10.1080/2331205X.2017.1302909

13. Hąc-Wydro, K., Flasiński, M., Broniatowski, M., & Sołtys, M. (2017). Studies on the Behavior of Eucalyptol and Terpinen-4-ol—Natural Food Additives and Ecological Pesticides—in Model Lipid Membranes. Langmuir, 33(27), 6916-6924. doi:10.1021/acs.langmuir.7b00774

14. Kaur, G., Athar, M., & Alam, M. S. (2009). Eugenol precludes cutaneous chemical carcinogenesis in mouse by preventing oxidative stress and inflammation and by inducing apoptosis. *Molecular Carcinogenesis*,49(3), 290-301. doi:10.1002/mc.20601

15. Kim, D., Lee, H., Jeon, Y., Han, Y., Kee, J., Kim, H., & Hong, S. (2015). Alpha-pinene exhibits anti-inflammatory activity through the suppression of MAPKs and the NF-κB pathway in mouse peritoneal macrophages. *The American Journal of Chinese Medicine*, 43(04), 731-742. doi:10.1142/s0192415x15500457

16. Kozioł, A., Stryjewska, A., Librowski, T., Sałat, K., Gaweł, M., Moniczewski, A., & Lochyński, S. (2014). An overview of the pharmacological properties and potential applications of natural monoterpenes. *Mini Reviews in Medicinal Chemistry*, *14*(14), 1156–1168.

17. Kunkel, E. J., Plavec, I., Nguyen, D., Melrose, J., Rosler, E. S., Kao, L. T., … Berg, E. L. (2004). Rapid structure-activity and selectivity analysis of kinase inhibitors by BioMAP analysis in complex human primary cell-based models. *Assay and Drug Development Technologies*, *2*(4), 431–441. https://doi.org/10.1089/adt.2004.2.431

18. Lv, X. N., Liu, Z. J., Zhang, H. J., & Tzeng, C. M. (2013). Aromatherapy and the central nerve system (CNS): therapeutic mechanism and its associated genes. *Current Drug Targets*, *14*(8), 872–879.

19. Nam, S., Chung, C., Seo, J., Rah, S., Kim, H., & Jeong, H. (2014). The therapeutic efficacy of α-pinene in an experimental mouse model of allergic rhinitis. *International Immunopharmacology*, 23(1), 273-282. doi:10.1016/j.intimp.2014.09.010

20. Navarra, M., Mannucci, C., Delbò, M., & Calapai, G. (2015). Citrus bergamia essential oil: from basic research to clinical application. *Frontiers in Pharmacology*, *6*, 36. https://doi.org/10.3389/fphar.2015.00036

21. Pal, D., Banerjee, S., Mukherjee, S., Roy, A., Panda, C. K., & Das, S. (2010). Eugenol restricts DMBA croton oil induced skin carcinogenesis in mice: Downregulation of c-Myc and H-ras, and activation of p53 dependent apoptotic pathway. *Journal of Dermatological Science*, 59(1), 31-39. doi:10.1016/j.jdermsci.2010.04.013

22. Perry, N., & Perry, E. (2006). Aromatherapy in the management of psychiatric disorders: clinical and neuropharmacological perspectives. *CNS Drugs*, *20*(4), 257–280.

23. R Development Core Team. (2011). R: A language and environment for statistical computing. Vienna, Austria: the R Foundation for Statistical Computing. Retrieved from http://www.R-project.org/

24. Rehman, M. U., Tahir, M., Khan, A. Q., Khan, R., O., Lateef, A., & Sultana, S. (2014). D-limonene suppresses doxorubicin-induced oxidative stress and inflammation via repression of COX-2, iNOS, and NFκB in kidneys of Wistar rats. *Experimental Biology and Medicine*, 239(4), 465-476. doi:10.1177/1535370213520112

25. Rufino, A. T., Ribeiro, M., Sousa, C., Judas, F., Salgueiro, L., Cavaleiro, C., & Mendes, A. F. (2015). Evaluation of the anti-inflammatory, anti-catabolic and pro-anabolic effects of E-caryophyllene, myrcene and limonene in a cell model of osteoarthritis. *EuropeanJournal of Pharmacology*, 750, 141-150. doi:10.1016/j.ejphar.2015.01.018

26. Yoon, W.-J., Lee, N. H., & Hyun, C.-G. (2010). Limonene suppresses lipopolysaccharide-induced production of nitric oxide, prostaglandin E2, and pro-inflammatory cytokines in RAW 264.7 macrophages. *Journal of Oleo Science*, *59*(8), 415–421.

27. Zhou, J., Tang, F., Mao, G., & Bian, R. (2004). Effect of alpha-pinene on nuclear translocation of NF-kappa B in THP-1 cells. *Acta Pharmacologica Sinica*, *25*(4), 480–484.

Citation: **Xuesheng Han, Tyler Bahr,** *"Biological Activity of an Essential Oil Blend in Human Dermal Fibroblasts". American Research Journal of Dermatology. 1(1): 1-21.*